Characterization of Bimodal Coordination Structure in Nitrosyl Heme Complexes through Hyperfine Couplings with Pyrrole and Protein Nitrogens

A. M. Tyryshkin,[†,‡] S. A. Dikanov,*[,†,§] E. J. Reijerse,[∥] C. Burgard,[⊥] and J. Hüttermann[⊥]

Contribution from the Institute of Chemical Kinetics and Combustion, Novosibirsk 630090, Russia, Department of Molecular Spectroscopy, University of Nijmegen, Toernooiveld, 6525 ED Nijmegen, The Netherlands, and Fachrichtung Biophysik und Physikalische Grundlagen der Medizin, Universität des Saarlandes, 66421 Homburg/Saar, Germany

Received June 15, 1998. Revised Manuscript Received February 12, 1999

Abstract: *Orientation-selected* three-pulse ESEEM experiments have been performed on a series of nitrosyl hemoproteins: HbNO in its two quaternary (R/T) states, the isolated NO-ligated α(*β*)-chains of hemoglobin, two hybrids of hemoglobin with asymmetrically ligated α(*β*)-chains, NO−myoglobin, and NO−Fe^{2+}(TPP)−imidazole model complexes. The ESEEM spectra of the native complexes clearly revealed the contribution from two conformational states of the NO−heme group. At 4.2 K the αNO and *β*NO chains were found in an almost pure state, i.e., 80% "state I" and 90% "state II", respectively. These results correlate well with the two-conformation model of 6-coordinated NO−heme complexes proposed earlier from the evaluation of temperature-dependent EPR/ENDOR spectra (Morse, R. H.; Chan, S. I. *J. Biol. Chem.* **1980**, *255*, 7876. Hüttermann, J.; Burgard, C.; Kappl, R. *J. Chem. Soc., Faraday Trans.* **1994,** *90*, 3077). Application of two-dimensional ESEEM spectroscopy (HYSCORE) to the isolated αNO and *β*NO chains allowed the characterization of the pyrrole nitrogen HFI in both conformations. A third nitrogen coupling was identified in the HYSCORE of the *β*NO chain. It was tentatively assigned to the N_ϵ nitrogen of distal His E7 which is suggested to form a hydrogen bond to the NO group in the axial NO−heme conformation. These findings support the proposal that the variation of binding geometry in two states of NO−heme is controlled by the heme's protein surrounding and could provide an important contribution to the discussion on the physiological role of NO related to its interactions with protein metal centers.

Introduction

Nitrosyl (NO)-ligated hemoglobin (HbNO) is considered to be a useful model to provide insight into the biochemistry of oxyhemoglobin (HbO_2). Like oxyhemoglobin, HbNO exhibits cooperative effects of a mutual influence between various ligands reacting with α(*β*)-chains in tetrameric hemoglobin and undergoes quaternary structural changes which are comparable to the R−T transitions between oxy and deoxy states of hemoglobin.[1−4]

More recently, the discovery of NO biosynthesis in mammals and the versatile role of NO in physiological processes[5,6] has stimulated new interest in the properties of NO−protein interactions. For instance, NO can act as a neurotransmitter, a vasodilator, and a cytotoxic agent.[7,8] NO is synthesized from L-arginine on a heme site of a family of enzymes called nitric oxide synthases (NOSs) in endothelial cells, macrophages, neutrophils, and platelets.[9,10] This endogenous NO interacts with other heme and non-heme iron proteins performing various cellular inhibition and activation functions.[11] These findings are another stimulus to perform detailed spectral and structural studies of NO metal complexes in proteins, in particular heme−NO centers. Structural studies of NO interaction with the heme group and the surrounding protein moiety are of vital importance for the understanding of its biosynthesis and its physiological role.

The NO radical bound to the central Fe^{2+} ion in the hemoprotein forms a paramagnetic, low-spin ($S = {}^1/_2$) complex. Due to this property, EPR spectroscopy has been crucial in the study of NO interaction with hemoproteins[1,2,12−14] as well as its physiological role.[15,16] A number of EPR and electron−nuclear double-resonance (ENDOR) studies of NO−hemoglo-

* Present address for correspondence: Illinois EPR Research Center, University of Illinois at Urbana−Champaign, 190 MSB, 506 S. Matheus Avenue, MC-714, Urbana, IL 61801; (fax) (217) 333-8868; (e-mail) dikanov@uiuc.edu.

† Institute of Chemical Kinetics and Combustion.

‡ (25.06.1993-23.06.1994) NWO Grant 07-13-089.

§ (01.06.1992-31.10.1993) Alexander von Humboldt Foundation Research Fellow in Saarland University.

∥ University of Nijmegen.

⊥ Universität des Saarlandes.

(1) Perutz, M. F.; Kilmartin, J. V.; Nagai, K., Szabo, A.; and Simon, S. R. *Biochemistry* **1976,** *15*, 378.
(2) Maxwell, J. C., Caughey, W. C. *Biochemistry* **1976**, *15*, 388.
(3) Henry, Y.; Banerjee, R. *J. Mol. Biol.* **1973,** *73*, 469.
(4) Cassoly, R. *J. Mol. Biol.* **1975,** *98*, 581.
(5) Ignarro, L. J. *Annu. Rev. Pharmacol. Toxicol.* **1990,** *30*, 535.
(6) Butler, R. B.; Williams, D. L. H. *Chem. Soc. Rev.* **1993,** *22*, 233.
(7) Lancaster, J. R., Jr. *Am. Sci.* **1992,** *80*, 248.
(8) Snyder, S. H.; Bredt, D. S. Sci. *Am.* **1992,** *266*, 68.
(9) Kerwin, F. F., Jr.; Lancaster, J. R., Jr.; Feldman, P. L. *J. Med. Chem.* **1995,** *38*, 4343.
(10) Griffith, O. W.; Stuehr, D. J. *Annu. Rev. Physiol.* **1995,** *57*, 707.
(11) Henry, Y.; Lepoivre, M.; Drapier, J.-C.; Ducrocq, C.; Boucher, J.-L.; Guissani, A. *FASEB J.* **1993,** *7*, 1124.
(12) Morse R. H.; Chan, S. I. *J. Biol. Chem.*, **1980,** *255*, 7876.
(13) Hüttermann, J.; Burgard, C.; Kappl, R. *J. Chem. Soc, Faraday Trans.* **1994,** *90*, 3077.
(14) Deatherage, J. F.; Moffat, K. *J. Mol. Biol.* **1979,** *134*, 401.

10.1021/ja982085y CCC: $18.00
Published on Web 03/27/1999

Table 1. Description of the Investigated Samples, the Abbreviations Used, and the Equilibrium Weights for States I (Rhombic) and II (Axial) in Hemoglobin (Myoglobin) Compounds As Estimated from ESEEM Analysis at 4.2 K

sample abbrev	description	(n_β/n_α)	n_{I} (%)[a]	n_{II} (%)[a]
αNO	isolated NO-ligated α(β)-chains of hemoglobin		80	20
βNO			10	90
HbNO(R)	NO-ligated hemoglobin in the quaternary R(T) states	1.01	45	55
HbNO(T)		1.01	45	55
(αNO, βCO)Hb	two hybrids of hemoglobin with asymmetrically (NO,CO)-ligated α(β)-chains		80	20
(αCO, βNO)Hb		2.95	28	72
MbNO	NO-ligated myoglobin	0.71	51	49
NO−Fe^{2+}(TPP)−Im	NO−Fe^{2+}(tetraphenylporphyrin)−imidazole complexes with ^{14}N- or ^{15}N-substituted imidazoles			

[a] The fractions of states I and II are calculated from (n_β/n_α) ratios including the correction for the estimated compositions of αNO and βNO chains: $n_{\mathrm{I}} = 0.7n_\alpha + 0.1$. The error margin is ∼25%.

bin, its isolated α- and β- subunits, myoglobin, and several model compounds such as NO-ligated Fe−tetraphenylporphyrin (TPP) with imidazole as sixth axial ligand were performed in frozen solutions[2,3,12,13,17−22] as well as in single crystals[23−26] aiming at an elucidation of structural details of the NO−hemoglobin interactions. While these studies have contributed to the understanding of the electronic structure and geometry of the NO-bound species, several details, especially those concerning changes upon R−T-"like" transitions, still remain unclear.[27,28] In part, the lack of more definitive conclusions is due to the difficulty of an unambiguous interpretation of the EPR and the rather complex ENDOR spectra of these species.

The EPR and ENDOR investigations have yielded information about the *g*-tensor principal components, nitrogen hyperfine couplings of axial ligands, and proton interactions of the porphyrin moiety and surrounding protein. The reported hyperfine couplings for the nitrogen of nitric oxide (30−50 MHz) and for the coordinated nitrogen of the proximal histidine (or imidazole in model complexes) of 15−20 MHz are large enough to be well observable in ENDOR[20,21] and even partially in the EPR spectra of frozen solutions.[3,12,19] ENDOR technique specifically demonstrates high resolution in the study of weakly coupled protons. However, EPR and ENDOR were ineffective in the detection of couplings from pyrrole nitrogens, which form the equatorial coordination of heme iron. For nitrosyl heme proteins and model compounds, these couplings were only observed using pulsed EPR techniques, i.e., electron spin−echo envelope modulation (ESEEM) spectroscopy.[29,30] This technique has been successfully applied for the last twenty years in the study of active metal sites in metalloproteins.[31,32]

The application of ESEEM spectroscopy to the nitrosyl hemoproteins and model compounds has confirmed the theoretical prediction[33] that hyperfine couplings with the pyrrole nitrogens should give rise to nuclear spin frequencies of ≤5.5 MHz. From a qualitative comparison of the ESEEM spectra of NO-ligated hemoglobin A, isolated NO−α(β)-chains of hemoglobin, and NO−Fe(TPP)−(pyridine or imidazole) model complexes, Magliozzo et al.[30] had concluded that only one type of pyrrole nitrogen contribute to the ESEEM in six-coordinated NO−heme complexes with magnetic couplings similar in all proteins and models investigated. These conclusions, however, were based on studies without systematic orientation selection.

Previous EPR/ENDOR studies converged into a "two-state" model of the structural dynamics of the various 6-coordinated Fe(NO)−porphyrin species. The original model derived from EPR for the two states involved differences in the displacement of the iron ion with respect to the heme plane.[12] More recent combined EPR and ENDOR studies associated one state with a tilted conformation in which the Fe−(NO) bond does *not* coincide with the normal to the porphyrin plane, whereas the other represents the more familiar axial arrangement.[13,24,28] It turns out that the EPR/ENDOR spectra of both native and model compounds can be described in terms of these two basic states. One should note, however, that both the spectra characteristics detected in EPR and the relative contributions of the two states to the sum spectrum are temperature dependent.[13]

In the present work, we investigate whether the same two-state model is applicable to the ESEEM spectra and, if so, how it is reflected in the pyrrole nitrogen couplings. This in turn, will lead to a more complete structural characterization of the two states of nitrosyl−heme complexes.

Orientation-selected ESEEM experiments have been performed on a series of nitrosyl hemoproteins given in Table 1 and model NO−Fe(TPP)−imidazole complexes. The 1D ESEEM ^{14}N signals are interpreted in terms of the contribution of two types of nitrogens, which are present in all samples but have varying relative intensity ratios. Subsequent application of 2D frequency-correlation spectroscopy (HYSCORE) to the NO-ligated α- and β-chains has provided further evidence of the two nonequivalent nitrogens as well as the identification of a third type of nitrogen. The HFI and NQI parameters of these nitrogens have been determined for the first time, and their assignment to specific nitrogens of the heme−protein moiety will be discussed.

(15) Henry, Y. A.; Guissani, A.; Ducastel, B. *Nitric oxide research from chemistry to biology: EPR spectroscopy of nitrosylated compounds;* Landes Bioscience: Austin, TX, 1997.
(16) *Methods in nitric oxide research*; Feelisch, M., Stamler, J. S., Eds.; Wiley: Chichester, 1996; Chapters 23−25.
(17) Shida, T.; Hwang, K.-J.; Tyuma, I. *Biochemistry* **1969**, *8*, 378.
(18) Rein, H.; Ristau, O.; Scheler, W. *FEBS Lett.* **1972,** *24*, 24.
(19) Nagai, K.; Hori, H.; Yoshida, S.; Sakamoto, H.; Rokimoto, H. *Biochim. Biophys. Acta* **1978,** 532, 17.
(20) LoBrutto, R.; Wei, Y.; Mascarenhas, R.; Scholes, C. P.; King, T. E. *J. Biol. Chem.* **1983,** *258*, 7437.
(21) Höhn, M.; Hüttermann, J.; Chien, J. C. W.; Dickinson, L. C. *J. Am. Chem. Soc.* **1983,** 105, 109.
(22) Yoshimura, T. *Inorg. Chim. Acta* **1986,** *125*, L27.
(23) Chien, J. C. W. *J. Chem. Phys.* **1969,** *51*, 4220.
(24) Hori, H.; Ikeda-Saito, M.; Yonetani, T. *J. Biol. Chem.* **1981,** *256*, 7849.
(25) Utterback, S. G.; Doetschman, D. C.; Szumowski, J.; Rizos A. K. *J. Chem. Phys.* **1983,** 78, 5874.
(26) Kappl, R.; Hüttermann, J. *Isr. J. Chem.***1989,** *29*, 73.
(27) Kappl, R.; Hüttermann, J. In *Advanced EPR. Applications in Biology and Biochemistry;* Hoff, A. J., Ed.; Elsevier: Amsterdam, 1989; p 501.
(28) Hüttermann, J. In *Biological Magnetic Resonance, Volume 13: EMR of Paramag*netic Molecules; Berliner, L. J., Reuben, J., Eds.; Plenum Press: New York, 1993; p 219.
(29) Peisach, J.; Mims, W. B.; Davis, J. L. *J. Biol. Chem.* **1979,** *254*, 12379.
(30) Magliozzo, R. S.; McCracken, J.; Peisach, J. *Biochemistry* **1987**, *26*, 7923.
(31) *Advanced EPR. Applications in Biology and Biochemistry*; Hoff, A. J., Ed.; Elsevier: Amsterdam, 1989; Chapters 1−6.
(32) Dikanov, S. A.; Tsvetkov, Yu. D. *Electron Spin−Echo Envelope Modulation (ESEEM) Spectroscopy*, CRC Press: Boca Raton FL, 1992.
(33) Mun, S. K.; Chang, J. C.; Das, T. P. *Proc. Natl. Acad. Sci. U.S.A.* **1979,** *76*, 4842.

Experimental and Methods

Sample Preparation. The model complexes and the native NO−heme materials were prepared as described elsewhere.[13] All samples (Table 1) were transferred immediately after preparation into EPR sample tubes (Spintec) and were frozen and stored in liquid nitrogen. Typical sample volumes were 200−300 μL.

Pulsed EPR Spectroscopy. ESEEM experiments were performed on an X-band pulsed EPR spectrometer Bruker ESP 380 using an overcoupled dielectric resonator. The magnetic field was measured with a Bruker NMR gaussmeter (ER-035M), and the microwave frequency was determined with a digital frequency counter. All measurements were carried out at 4.2 K using an Oxford CF 935 cryostat.

1D ESEEM patterns were obtained using the three-pulse stimulated experiment ($\pi/2-\tau-\pi/2-T-\pi/2-\tau-$echo) with τ held constant and T varied. 2D HYSCORE experiments employed the ($\pi/2-\tau-\pi/2-t_1-\pi-t_2-\pi/2-\tau-$echo) pulse sequence, where the echo is measured as a function of t_1 and t_2. A total of 256 points were measured in each dimension with an increment of 24 ns. Both techniques were used with appropriate phase cycling to eliminate unwanted echoes.[34,35] The length of the $\pi/2$ pulses was 16 or 24 ns. The π-inversion pulse in the HYSCORE experiment was 32 ns and of the same amplitude as $\pi/2$ pulses. There was no advantage to use a strong narrow π-pulse in our experiments because a 32-ns pulse was nonselective enough to exite all allowed and forbidden transitions of the electron nitrogen spin system. The spectrometer dead time was (τ + 24) ns.

Prior to Fourier transformation (FT) the time-domain 1D ESEEM patterns were normalized to unity background by fitting the relaxation decays on splines (or polynomials of different degrees) followed by division of the experimental time-domain pattern by the fitted baseline decay. No attempts were made to reconstruct points missing from time-domain ESEEM data due to spectrometer dead time. All 1D FT-ESEEM spectra shown are in magnitude mode.

2D HYSCORE spectra were treated using commercial software (WinEPR). The background decay in both dimensions (t_1, t_2) was subtracted using a polynomial fit followed by apodization with a Hamming window and zero-filling to 512 points in each dimension. Then FT was applied in two dimensions. The spectra shown are contour plots in magnitude mode with logarithmic scaling of the contour levels.

Analysis of ^{14}N Powder 1D ESEEM Spectra. For ^{14}N nuclei (nuclear spin $I = 1$) there are three nuclear transitions ν_{kn+} and ν_{lm-} between three nuclear sublevels (k, n, and l, $m = 1, ..., 3$) in each electron spin manifold ($\pm$) adding up to six nuclear transitions in total. For simplicity, the lower frequency transitions ($\nu_{12\pm}$ and $\nu_{23\pm}$) between the adjacent sublevels are usually called single-quantum (sq) transitions whereas the higher frequency one ($\nu_{13\pm}$) between the outer sublevels is referred to as the double-quantum (dq) transition.[1] Strictly, these definitions are only valid when the nuclear quadrupole term of the nuclear spin Hamiltonian is negligible in comparison to the other terms, i.e., the nuclear Zeeman interaction and hyperfine interaction. The nuclear spin projections (m_I) on the direction of the applied magnetic field are then good quantum numbers of the nuclear substates. In this case the single-quantum transition corresponds to $\Delta m_I = 1$ and the double-quantum transition to $\Delta m_I = 2$. However, these nuclear spin projections are no longer good quantum numbers when the NQI term becomes significant. In the latter case, the nuclear eigenfunctions are superposition of nuclear states with different projections $\sum a_m|m\rangle$, and for instance, the double-quantum transition would merely correspond to a transition between the levels whose most abundant nuclear states are different by $\Delta m_I = 2$. Usually, only a subset of the six nuclear transitions is visible in experimental ESEEM spectra.[32]

It has been demonstrated both theoretically and experimentally[36,37] that the relative magnitude of the nuclear Zeeman frequency (ν_I) and the (isotropic) hyperfine interaction of the nitrogen nucleus plays a key role in the interpretation of one-dimensional ESEEM powder spectra. Two types of powder ESEEM patterns are usually distinguished. In the case of dominant (isotropic) hyperfine interaction ($|a|2 \gg \nu_I$), the two double-quantum transitions $\nu_{dq\pm}$ give rise to sharp peaks in the spectrum. To a good accuracy, their position is given by[36,37]

$$\nu_{dq\pm} = 2[(\nu_I \pm a/2)^2 + K^2(3 + \eta^2)]^{1/2} \quad (1)$$

The single-quantum transitions from both electron spin manifolds have a significant anisotropic line broadening and usually do not produce noticeable intensity in the spectrum.

For another range of Zeeman and hyperfine interactions, three intense narrow lines satisfying the relation of additivity characterize the three-pulse ^{14}N ESEEM spectra. This regime corresponds to the so-called "cancellation condition" indicating that the external magnetic field approximately cancels the local hyperfine field at the nucleus in one electron spin manifold, i.e., $(\nu_I - a/2) \cong 0$.[36,37] The observed ESEEM lines correspond to the pure quadrupole frequencies ('NQI' lines):

$$\nu_0 = 2K\eta, \quad \nu_- = K(3 - \eta), \quad \nu_+ = K(3 + \eta) \quad (2)$$

where $K = e^2Qq/4h$ is the quadrupole coupling constant and $\eta = (Q_{xx} - Q_{yy})/Q_{zz}$ the asymmetry parameter. The three NQI peaks are often accompanied by the $\nu_{dq\pm}$ line (eq 1) from the second electron spin manifold in which the local hyperfine field *adds* to the applied magnetic field. The transition between these two types of powder ESEEM patterns occurs when[37]

$$|\nu_I \pm a/2| \sim 2/3K \quad (3)$$

Interpretation of ^{14}N HYSCORE Spectra. After 2D-FT of the (real) time domain (t_1,t_2) measured in HYSCORE experiment, a 2D frequency domain is obtained showing only correlations (ν_{kn+}, ν_{lm-}) between nuclear spin frequencies of opposite electron spin m_S manifolds.[35,38,39] This property significantly simplifies the analysis of congested spectra due to interactions of a large number of nonequivalent nuclei.[40,41] Nine pairs of cross-peak features can occur between the six nuclear spin frequencies of the nitrogen nuclei including one dq−dq correlation (ν_{dq+}, ν_{dq-}), four dq−sq correlations ($\nu_{dq+/-}$, $\nu_{sq-/+}$), and four sq−sq correlations ($\nu_{sq+/-}$, $\nu_{sq-/+}$). In addition, it turns out that the cross-peak intensities in the two quadrants (+,+) and (+,−) of the 2D frequency domain will be different for the related features; i.e., the ($+\nu_1$, $+\nu_2$) feature will have an intensity different from that of the ($+\nu_1$, $-\nu_2$) feature.[35,39] Analytical expressions for the cross-peak intensities have only been obtained for the case $S = {}^1/_2$, $I = {}^1/_2$ (e.g. proton HYSCORE).[35] The peculiarities of nitrogen HYSCORE spectra are, however, extensively described in the available experimental[40−46] and simulated[42−44] 2D spectra. Two particular types of 2D powder patterns are usually observed, one of which corresponds to the strong hyperfine coupling regime ($|a|/2 \gg \nu_I$) while the other is linked to the cancellation condition ($|a|/2 \cong \nu_I$). In the case of strong hyperfine coupling, the dominating feature of the spectra is the dq−dq correlation developing in the (+,−) quadrant.[40−44] The cross-peak pattern becomes very different in the case of the cancellation condition.[43,45,46] Here, most

(34) Fauth, J.-M.; Schweiger, A.; Braunschweiler, L.; Forrer, J.; Ernst, R. R. *J. Magn. Reson.* **1986,** 66, 74.
(35) Gemperle, C.; Aebli, G.; Schweiger, A.; Ernst, R. R. *J. Magn. Reson.* **1990,** *88*, 241.
(36) Astashkin, A. V.; Dikanov, S. A.; Tsvetkov, Yu. D. *J. Struct. Chem.* **1984**, *25*, 200.
(37) Flanagan, H. L.; Singel, D. J. *J. Chem. Phys.* **1987**, *87*, 5606.
(38) Höfer, P.; Grupp, A.; Nebenführ, H.; Mehring, M. *Chem. Phys. Lett.* **1986**, *132*, 279.
(39) Shane, J.; Höfer, P.; Reijerse, E. J.; de Boer; E. *J. Magn. Reson.* **1992,** *99*, 596.
(40) Dikanov, S. A.; Samoilova, R. I.; Smieja, J. A.; Bowman, M. K. *J. Am. Chem. Soc.* **1995,** *117*, 10579.
(41) Buy, C.; Matsui, T.; Andrianambinintsoa, S.; Sigalat, C.; Girault, G.; Zimmermann, J.-L. *Biochemistry* **1996**, *35*, 14281.
(42) Reijerse, E. J.; Shane, J. J.; de Boer, E.; Höfer, P.; Collison, D. In *Electron Magnetic Resonance of Disordered Systems*; Yordanov, N. D., Ed.; World Scientific: Singapore, 1991; p 253.
(43) (a) Dikanov, S. A.; Xun, L.; Karpiel, A. B.; Tyryshkin, A. M.; Bowman, M. K. *J. Am. Chem. Soc.* **1996**, *118*, 8408. (b) Dikanov, S. A.; Davydov, R. M.; Gräslund, A.; Bowman, M. K. *J. Am. Chem. Soc.* **1998**, *120*, 6797.
(44) Reijerse, E. J.; Tyryshkin, A. M.; Dikanov, S. A. *J. Magn. Reson.* **1998,** *131*, 295.
(45) Kofman, V.; Farver, O.; Pecht, I.; Goldfarb, D. *J. Am. Chem. Soc.* **1996,** *118*, 1201.
(46) van Dam, P. J.; Reijerse, E. J.; Hagen, W. R. *Eur. J. Biochem.* **1997**, *248*, 355−361.

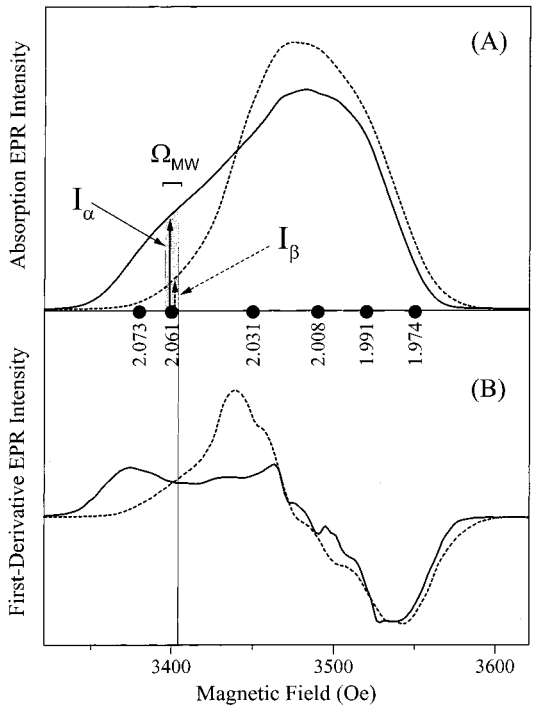

Figure 1. Absorption (A) and first-derivative (B) EPR spectra of isolated αNO and *β*NO chains of hemoglobin measured at 15 K. The points indicate the magnetic field positions (effective *g*-factors) where ESEEM measurements were carried out. The absorption EPR spectra are normalized for unit area, and the labels $I_{\alpha(\beta)}$ are used to represent their normalized EPR intensities. The shaded area under the absorption spectrum of the isolated αNO chains represents schematically the number of paramagnetic species excited by microwave pulses in orientation-selected ESEEM experiment. Ω_{MW} is the excitation bandwidth of the MW pulses.

intensity is shifted to the (+,+) quadrant of the spectra. The correlations between the NQI lines (eq 2) and the transitions from the opposite manifold appear as relatively weak ridges parallel to the f_1 and f_2 axis. This is because the NQI peaks are isotropic while the transition frequencies from the opposite manifold are usually orientation dependent. The ν_{dq+} peak, which has the lowest anisotropy, gives rise to the strongest correlation features.

Results

Figure 1 shows the absorption (A) and first-derivative (B) EPR spectra of isolated αNO and *β*NO chains of hemoglobin. The spectra exhibit a pronounced anisotropy of the electron *g*-tensor and are significantly different, especially in the low-field region ($g > 2.031$). In previous X- and Q-band EPR measurements,[1,2,12−14] the rhombic *g*-tensor (2.07, 2.004, 1.97) was ascribed to isolated αNO chains, and the nearly axial *g*-tensor (2.03−2.04, ∼1.99) was found for isolated *β*NO chains. The EPR spectra of the other samples investigated (Table 1) resemble the spectra of isolated αNO and *β*NO chains with a similar spread of the effective *g*-factors between 2.07 and 1.97. Orientation-selected ESEEM measurements were performed at different magnetic field settings along the powder EPR line shapes (indicated by filled circles in Figure 1A). At each magnetic field, the microwave pulses during the ESEEM experiment will excite only a small fraction of the paramagnetic species (illustrated in Figure 1 by a shaded area under the absorption EPR spectrum of isolated αNO chains). Only this fraction with its specific ("selected") set of orientations with respect to the direction of the applied magnetic field is monitored.[47] To facilitate the comparison of ESEEM spectra of the different samples, orientation-selected ESEEM experiments for all samples were performed with the microwave frequency adjusted to the same value of 9.809 ± 0.002 GHz and at the same set of magnetic fields (3380, 3400, 3450, 3490, 3520, 3550 G) which corresponds to the following set of effective *g*-values: (2.073, 2.061, 2.031, 2.008, 1.991, and 1.974, respectively).

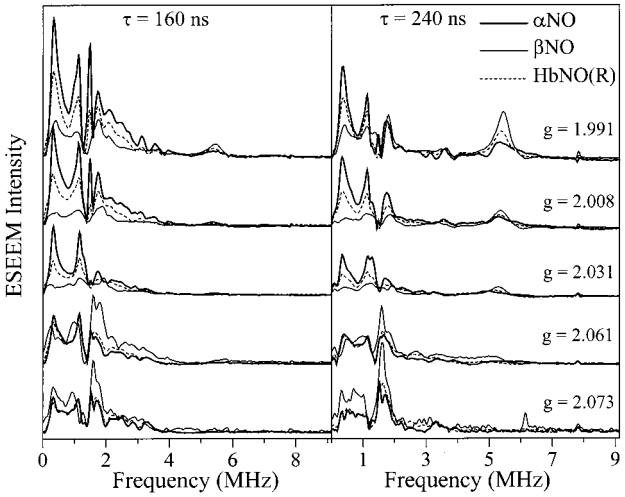

Figure 2. Experimental stimulated (three-pulse) FT-ESEEM spectra of isolated α(*β*)NO chains of Hb and of HbNO in its R-state recorded for two different *τ*-values and at five different magnetic fields corresponding to the shown *g*-values. See Experimental Section for the other experimental conditions.

Three-Pulse 1D ESEEM Spectra. Figure 2 depicts the three-pulse FT-ESEEM spectra in the frequency region 0−9 MHz for the three samples: NO−hemoglobin in the quaternary R-state and the isolated αNO and *β*NO chains. The spectra shown were recorded at two different *τ*-values and at five different effective *g*-values across the EPR powder line shapes. The spectra exhibit a complex line shape with many lines of different degrees of resolution. These lines can only be ascribed to interactions with ^{14}N nuclei from the surrounding of the heme iron. Taking into account the previous EPR, ENDOR, and ESEEM investigations of nitrosyl hemoglobins and their models,[20,21,29,30] one is led to expect that the pyrrole heme nitrogens give the main contribution in this spectral region. Although the spectral features clearly vary as a function of the field position within the EPR powder spectrum, thus indicating effective orientation selection, the main differences are observed in line *intensities* and *shapes* rather than in line *positions*. At every magnetic field and for both *τ*-values, the low-frequency lines (<3 MHz) are more developed in the spectra of the αNO sample, whereas a high-frequency line (∼5.5 MHz) is more dominant in the spectra of *β*NO. The spectra of HbNO in R-state show intermediate line intensities in these two frequency regions.

The points of intermediate ($g_2 = 2.002$) and minimum ($g_3 = 1.979$) principal values of the electron *g*-tensor are not very effectively separated in the X-band frozen solution spectra. The difference $|g_2 - g_3| \approx 0.02-0.03$ corresponds to a field range of only 35−50 G. In addition, the significant spread of intrinsic EPR line shape created by the hyperfine structure due to nitric oxide ($a_{iso} \cong 17.1$ G) and histidine ($a_{iso} \cong 6.2$ G) nitrogens[27] leads to further admixture of g_2 orientations into g_3 spectra, and vice versa. Consequently, very similar ENDOR patterns were usually detected for hemoproteins at the g_2 and g_3 points of

(47) Hoffman, B. M.; Martinsen, J.; Venters, R. A. *J. Magn. Reson.* **1984**, *59*, 110.

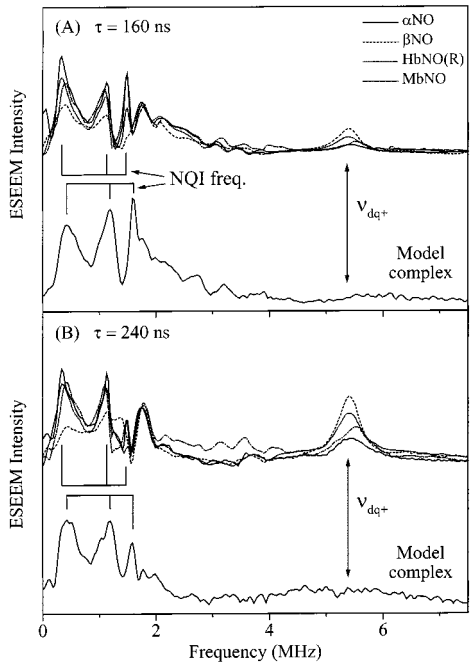

Figure 3. Comparison of experimental stimulated FT-ESEEM spectra of native and model NO−heme complexes measured at the high-field position of the EPR spectra ($g = 1.991$) at (A) $\tau = 160$ ns and (B) $\tau = 240$ ns. Experimental conditions are the same as for the ESEEM spectra in Figure 2.

powder EPR spectra.[13,27] Likewise, only very small differences are seen between the ESEEM spectra recorded in the ($g_2 - g_2$) region at the high-field edge of the EPR spectra ($g = 2.008$ and 1.991 in Figure 2). Since a broad set of orientations around the two principal directions of the g-tensor is expected to contribute to the ESEEM spectra in this region, it seems more appropriate to perform their qualitative analysis using approaches developed for powder rather than for single-crystal-like spectra.

In the ESEEM spectra from the high-field region, especially at $\tau = 160$ ns, one observes three narrow lines with frequencies of 0.33, 1.18, and 1.51 (±0.02) MHz satisfying the relation of additivity. The same set of lines is also observed in the spectra of all the other native samples (see Figure 3). The high intensity and narrow line width of these lines are typical for nitrogen nuclei in the regime of the cancellation condition (cf. eq 2). In this case, the three lines correspond to the nuclear quadrupole transition frequencies (NQI lines), and using eq 2, one can estimate quadrupole parameters $K = 0.45$ MHz and $\eta = 0.37$ for the protein samples.

Following Magliozzo et al.,[30] the 6-coordinated NO−Fe^{2+}-(TPP)−imidazole model complex with ^{14}N- and ^{15}N-enriched imidazole was also studied. Again the ESEEM spectra of both ^{14}N- and ^{15}N-ligated complexes demonstrate pronounced orientation dependence and, at the same time, show a close similarity to each other at all field positions. The spectra of the model complexes in the ($g_2 - g_3$) region also show three well-developed sharp lines; however, their frequencies, 0.43, 1.19, and 1.61 (±0.02) MHz, are slightly different from those observed in the spectra of the native samples (cf. Figure 3). It is remarkable that all native NO compounds including HbNO in two different R(T) quaternary states, separate α(β)NO chains, the two hybrids, and MbNO are characterized by the same set of NQI frequencies which, however, differ noticeably from the NQI frequencies of the model complexes. This difference, which exceeds the resolution of the ESEEM spectra in our study, was not reported previously.[30] Using eq 2, the quadrupole parameters $K = 0.47$ MHz and $\eta = 0.45$ are evaluated for the model complexes. The difference in NQI frequencies between the native and model systems is apparently due mainly to variation in the asymmetry parameter.

Since the isotopic substitution of both nitrogens in the imidazole ligand of the model complex does not influence the ESEEM spectra, they must be ascribed to interactions with the pyrrole nitrogens only. The three narrow lines observed in the ESEEM spectra of the ($g_2 - g_3$) region correspond then to the NQI frequencies of the pyrrole nitrogens. By analogy, the three slightly shifted lines observed in the spectra of the protein samples are assigned to the NQI frequencies of the heme pyrrole nitrogens as well. Support for this assignment comes from comparing the NQI parameters with those previously reported for pyrrole ^{14}N nitrogens in other metal complexes. Single crystals of Cu(TPP) give values $K = 0.463$ MHz and $\eta = 0.337$,[48] Ag(TPP) exhibits (0.457 MHz/0.513)[48] while VO(TPP) complexes in frozen solution have (0.47 MHz/0.5−0.6).[49] This comparison also demonstrates a high stability of the quadrupole coupling constant of pyrrole nitrogens and a broader variation of the asymmetry parameter with the chemical structure and surrounding matrix.

The ESEEM spectra of the native samples in the ($g_2 - g_3$) field region develop also additional lines at frequencies 1.7−1.8 and 5.3−5.5 MHz (best observed for $\tau = 240$ ns) and a weakly resolved set of lines between 2 and 4 MHz (Figure 2). In contrast to the NQI lines, the position of these peaks is not invariant over the different native samples. However, their intensities still show the same τ-dependence and a similar well-pronounced variation as a function of the applied magnetic field. A striking difference is observed between the proteins and the model complexes. The peak in the range 5.3−5.5 MHz is completely absent in the latter systems (Figure 3). A similar situation probably occurs for the 1.7−1.8-MHz region although some features of weak intensity are also present in the model systems.

In the previous study,[30] the line at 5.5 MHz was also observed for one of the model complexes, 6-coordinated NO−Fe^{2+}(TPP) complex with ^{14}N- and ^{15}N-labeled pyridine as sixth ligand, and assigned to double-quantum transition ν_{dq+} of the same set of pyrrole nitrogens that generate the strong NQI lines. However, such an assignment appears to be improbable because of the uncorrelated variation of relative intensities of the NQI lines and the 5.5-MHz line in the spectra of different samples (cf. Figure 2). The 5.5-MHz line is not observed for the model complex with imidazole axial ligand. This implies rather that the two sets of lines, i.e., NQI lines and 5.5-MHz line, belong to two different groups of nitrogens and that the variations of relative line intensities are just a reflection of the varying contribution of these two nitrogens to the ESEEM signal (see below**)**. To support this analysis, we have performed two-dimensional HYSCORE experiments on the αNO and βNO samples.

HYSCORE Spectra. HYSCORE spectra were measured at several g-values. The best signal-to-noise ratio and spectral resolution were obtained for the field position 3470 G ($g_{eff} = 2.007$). Figure 4 shows the HYSCORE spectra of the αNO (Figure 4A) and βNO (Figure 4B) subunits measured at this field with $\tau = 200$ ns. The two spectra display a similar set of cross-features, but the intensities are very different. As is seen

(48) Brown, T. G.; Hoffman, B. M. *Mol. Phys.* **1980,** *39,* 1073.
(49) Fukui, K.; Ohya-Nishiguchi, H.; Kamada, H. *J. Phys. Chem.* **1993,** *97,* 11858.

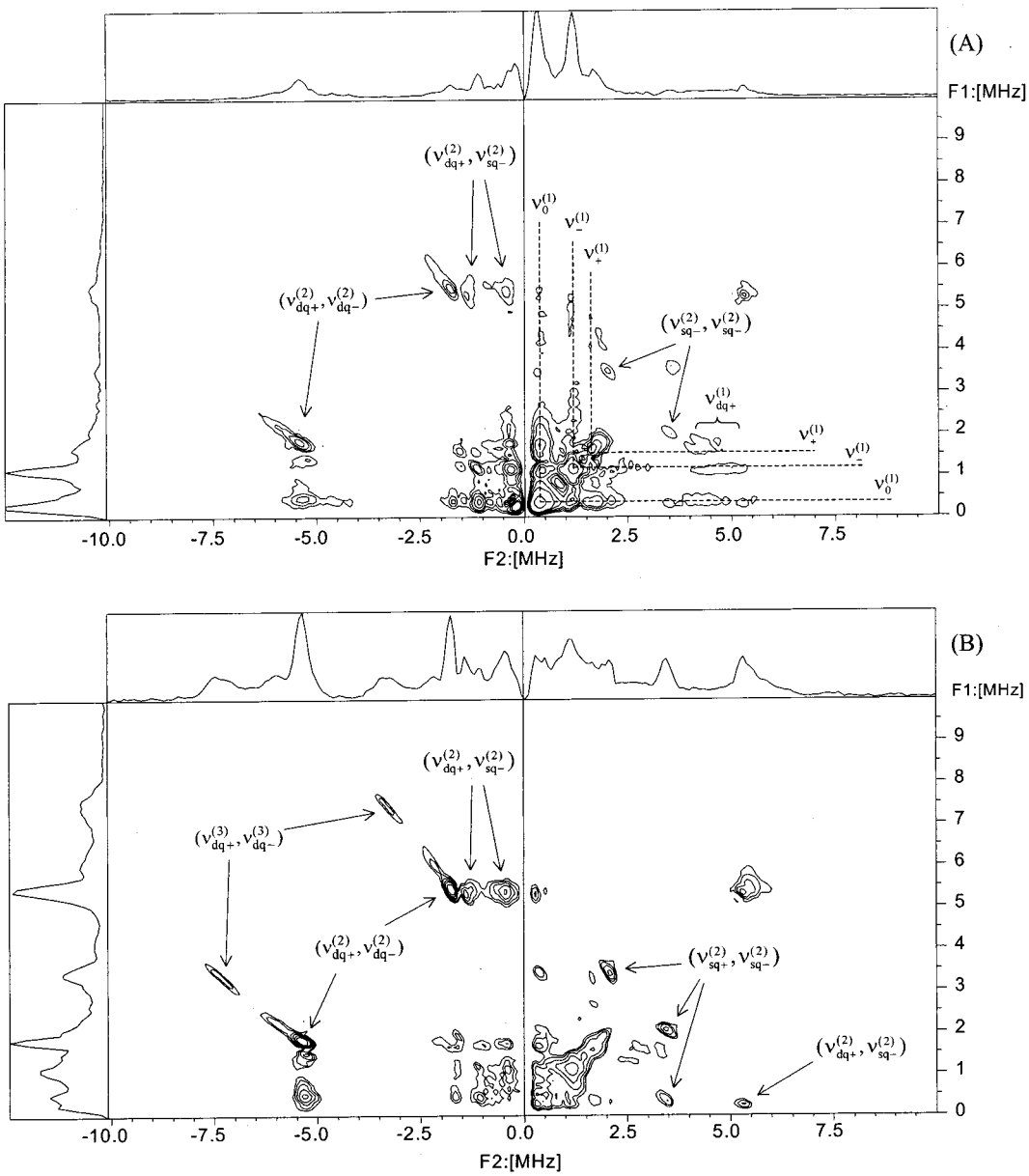

Figure 4. HYSCORE spectra of (A) αNO chains and (B) βNO chains of hemoglobin measured at $g_{\text{eff}} = 2.007$ (3470 G) and $\tau = 200$ ns. See Experimental Section for the other experimental conditions.

from the skyline projections, the most intense lines are located in the (+,+) quadrant for the αNO chains and in the (+,−) quadrant for the βNO subunits.

In the αNO spectrum, the three most intense peaks lie along the diagonal in the (+,+) quadrant and correspond to the three NQI lines 0.33, 1.18, and 1.51 MHz found in the three-pulse ESEEM spectra (Figure 2). In general, no diagonal peaks should be observed in HYSCORE spectra. However, they are often observed in experimental spectra because of incomplete inversion of electron spin magnetization by the π-pulse. Complete inversion of all electron spins is experimentally difficult to achieve due to inhomogeneous microwave field over sample size. In Figure 4A, these frequencies are indicated by dashed lines marked as $\nu_0^{(1)}$, $\nu^{(1)}$, and $\nu_+^{(1)}$, where the superscript refers to the type of (pyrrole) nitrogen N1. The intense diagonal peaks are accompanied by extended ridges running parallel to the f_1 and f_2 axis in the (+,+) quadrant of the spectrum. A symmetrical set of cross-features of lower intensity are also seen in the (+,−) quadrant. These ridges correlate the NQI lines with the single-quantum transitions $\nu_{\text{sq}+}^{(1)}$ of the same nitrogens from the opposite electron spin manifold. In addition, three straight-line segments are observed between 4 and 5 MHz in the (+,+) quadrant which can only be ascribed to the cross-correlation of the NQI lines with the double-quantum frequency $\nu_{\text{dq}+}^{(1)}$. Since the measurements were carried out at $g = 2.007$, a broad range of orientations contributes to the spectrum. This explains the extended character of the cross-peak ridges. At the same time, the ridges lie practically parallel to the f_1 and f_2 axis of the spectrum indicating a weak frequency dependence of the 0.33, 1.18, and 1.51 MHz lines at the different orientations. This supports their assignment to nitrogen nuclei near the cancellation condition. Using NQI parameters ($K = 0.45$ MHz, $\eta = 0.37$) estimated above from the NQI lines, the range of effective hyperfine couplings 1.55 MHz $< |a| <$ 2.77 MHz can be estimated from eq 3 to ensure nitrogens N1 to be in the cancellation condition. Then, eq 1 predicts double-quantum transition $\nu_{\text{dq}+}^{(1)}$ between 4.05 and 5.17 MHz. This estimation perfectly matches the cross-peak range 4.2−5.3 MHz in the αNO HYSCORE spectrum. No lines were observed in this frequency region in the three-pulse spectra of αNO, nor in the

Table 2. Nuclear Frequencies Observed in Three-Pulse ESEEM and HYSCORE Spectra, Their Assignment, and Estimated Quadrupole and Hyperfine Coupling Parameters of the Three Types of Nitrogen Nuclei (N1−N3) of Native and Model Nitrosyl−Heme Complexes

type of nitrogen	nuclear frequencies (MHz)		NQI parameters			HFI coupling (MHz)	paramagnetic species
	three-pulse ESEEM	HYSCORE	$K = e^2Qq/4h$ (MHz)	η	$P = K^2(3+\eta^2)$ (MHz^2)		
			Native Compounds				
N1	$[\nu_0^{(1)}, \nu_-^{(1)}, \nu_+^{(1)}] =$ [0.33, 1.18, 1.51]	$[\nu_0^{(1)}, \nu_-^{(1)}, \nu_+^{(1)}] =$ [0.33, 1.15, 1.49]	0.45	0.37	0.63	1.75−2.92	state I
N2	$\nu_{dq+}^{(1)} = ?$	$\nu_{dq+}^{(1)} = 4.2-5.3$ $\nu_{sq-}^{(2)} = [0.38, 1.4]$ $\nu_{sq+}^{(2)} = [?, 3.43]$	−	−	0.6	3.06	state II
N3	$\nu_{dq-}^{(2)} = 1.7-1.8$ $\nu_{dq-}^{(2)} = 5.3-5.5$	$\nu_{dq-}^{(2)} = 1.8$ $\nu_{dq+}^{(2)} = 5.42$ $\nu_{dq-}^{(3)} = 3.3$ $\nu_{dq+}^{(3)} = 7.4$	−	−	0.47	5.13	state II
			Model Complexes				
N1	$[\nu_0^{(1)}, \nu_-^{(1)}, \nu_+^{(1)}] =$ [0.43, 1.19, 1.61]	n/a[b]	0.47	0.45	0.71	−	state I

[a] ? and −, designate nonobserved frequencies. The determined HFI and NQR couplings have an accuracy of ∼0.05 MHz. [b] Not available.

other native and model complexes (Figures 2 and 3). A broad line width and a resulting low intensity precluded observation of $\nu_{dq+}^{(1)}$ in the 1D ESEEM spectra. Nevertheless, this transition is still detectable in the 2D spectra. The cross-ridges extend from 4.2 to 5.3 MHz that corresponds to a broad distribution of the effective hyperfine coupling of the N1 nitrogens $|a| =$ 1.75−2.92 MHz. This high HFI distribution could be due to a significant anisotropic hyperfine interaction and/or to strains of the heme−iron structure which can also lead to considerable variation of isotropic hyperfine coupling of the pyrrole nitrogens.

The cross-features produced by the N1 nitrogens are also seen in the HYSCORE spectrum of βNO but they are significantly less intense (Figure 4B). On the other hand, there are additional cross-peaks in the spectrum of αNO which become dominant in the spectrum of βNO. These include the pairs of cross-peaks at (5.42, 1.8), (5.35, 1.42), and (5.4, 0.43) MHz in the (+,−) quadrant, and the peaks at (5.35, 0.35), (3.43, 0.4), (3.43, 2.08) MHz in the (+,+) quadrant. These cross-features definitelybelong to different nitrogen (N2) with frequencies 0.4, 1.4, and 1.8 and 2.0, 3.4 and 5.4 MHz in the two-electron spin manifolds. The HYSCORE spectra therefore clearly confirmed that the lines observed in the three-pulse spectra (the low-frequency NQI lines and the line at 5.5 MHz) are due to *different* nitrogens. In addition, the HYSCORE spectra provide the complete set of nuclear frequencies of N2. Only two of the frequencies at 1.8 and 5.5 MHz were clearly seen in the three-pulse spectra. The first-order analysis of these frequencies estimates an effective hyperfine coupling of ∼3.4 MHz. This value significantly deviates from the cancellation condition in eq 3. Consequently, the three low frequencies 0.4, 1.4, and 1.8 MHz cannot be considered as the NQI frequencies of the N2 nitrogen. Instead, eq 1 is applicable to the two double-quantum transitions $\nu_{dq\pm}$ 5.42 and 1.8 MHz. This provides an estimation of the effective hyperfine constant $|a| = 3.06$ MHz and also the quadrupole-related parameter $K^2(3+\eta^2) = 0.6$ MHz^2 for the N2 nitrogens.

A completely new pair of peaks (7.4, 3.3) MHz appears in the (+,−) quadrant of the βNO spectrum. We assign these peaks to the dq-dq correlation of the third type of nitrogen N3. This assignment is based on the location of the cross-peak in the (+, −) quadrant, their contour line shape, and the difference of the two correlated frequencies ($\nu_{dq+}^{(3)} - \nu_{dq-}^{(3)}$) which is close to $4\nu_I$ of the nitrogen nuclei. Using eq 1, an effective hyperfine coupling $|a| = 5.13$ MHz and quadrupole parameter $K^2(3 + \eta^2) = 0.47$ MHz^2 are estimated for N3. The fact that the N3 signal was not observed in the three-pulse ESEEM spectra could be due to the τ-suppression effect in combination with the weak and broad nature of the spectral feature. It has been established that ESEEM contributions of this type are usually better resolved in HYSCORE because this technique, in contrast to the 1D three-pulse experiment, is almost insensitive to dead-time effects.

The frequencies of couplings N1−N3 observed in the three-pulse and HYSCORE spectra as well as the estimated hyperfine and quadrupole parameters are summarized in Table 2. Later, we will discuss a detailed assignment of the three groups of nitrogens to the specific nitrogen atoms in the heme−iron moiety. Here, for the purpose of further spectral analysis, we reiterate that three different nitrogen interactions were found in the ESEEM and HYSCORE spectra. The first type (N1) is due to the pyrrole nitrogens showing the smallest hyperfine coupling $|a| = 2.3 \pm 0.6$ MHz and producing the three prominent NQI lines in the three-pulse ESEEM spectra. The second (N2) and third (N3) interactions are yet to be assigned and can be characterized by larger hyperfine interaction ($|a| = 3.06$ and 5.13 MHz) leading to the double-quantum transitions $\nu_{dq\pm}^{(2)} =$ (5.42, 1.8) and $\nu_{dq\pm}^{(2)} =$ (7.4, 3.3) MHz, respectively.

Two-State Model for ESEEM Spectra of Heme Proteins. The observation of three sets of nitrogen couplings (in both three-pulse ESEEM and HYSCORE) of which the spectral contributions clearly varies between the αNO and βNO chain, suggests the involvement of at least two structurally different paramagnetic species. The αNO chain spectra are dominated by the N1 signals (i.e., the NQI lines) and should be closely associated with one of the species (state I). The βNO chain spectra are characterized by the contribution of N2 (i.e., the 5.5-MHz line in three-pulse ESEEM) associated with a different structure of the heme moiety (state II). The spectra of the other native samples show significant contribution of both N1 and N2 signals. They are interpreted as a mixture of two states. Assuming that the lines of nitrogens N1 and N2 identify weight contribution of two-state states, we tried to model the three-pulse ESEEM spectra of the native samples as a linear combination of the αNO and βNO chain spectra. The experimental time-domain envelopes for αNO and βNO chains ($V_{\alpha,\beta}$) were summed with appropriate coefficients $n_{\alpha,\beta}$:

$$V = n_\alpha V_\alpha + n_\beta V_\beta \tag{4}$$

then Fourier transformation was performed. Although the αNO

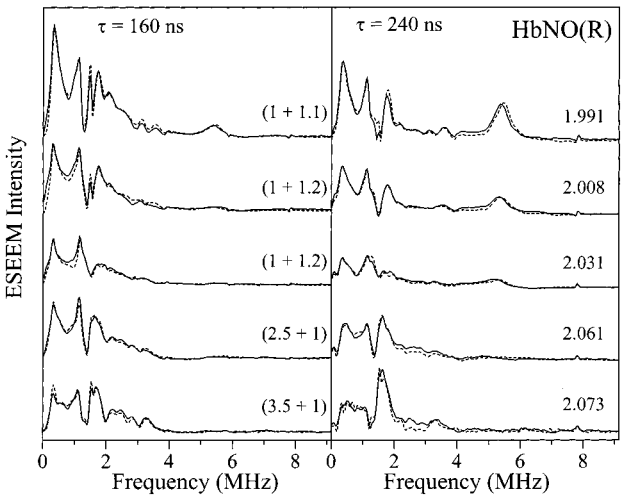

Figure 5. Stimulated FT-ESEEM spectra of HbNO in R-state: (solid lines) experimental and (dashed lines) calculated according eq 4 as a superposition of the corresponding experimental ESEEM spectra of αNO and *β*NO. The sums ($n_\alpha + n_\beta$) represent the weights of experimental α(*β*)NO spectra taken to produce the best correspondence of the simulated superposition to the respective experimental spectrum (see also Table 3).

Table 3. Contributions $n_\alpha + n_\beta$ of Experimental α/*β*NO Chain Spectra Used To Reconstruct the Three-Pulse ESEEM Spectra of Native Compounds (See Figure 5)

	g-value				
	1.991	2.008	2.031	2.061	2.073
HbNO(R/T)	1 + 1.1	1 + 1.2	1 + 1.2	2.5 + 1	3.5 + 1
(αCO,*β*NO)Hb	1 + 4.4	1 + 3.5	1 + 3.2	1 + 1.2	1.2 + 1
MbNO	1.5 + 1	1.3 + 1	1 + 1	4 + 1	

and *β*NO chains are definitely not in a pure structural state, we can still use the corresponding ESEEM spectra as a basis because, as apparent from Figure 2, the state I and II contributions attain extreme values for these species. An example of this procedure is presented in Figure 5 where the HbNO(R) spectra are reconstructed from the corresponding α- and *β*-chain spectra according to eq 4. For each magnetic field the n_α and n_β contributions are indicated. As expected, the ESEEM spectra for the two τ-values could be reconstructed using identical ratios. The correspondence between the experimental and reconstructed spectra is extremely good. Similar results were obtained for the other complexes (spectra available as complementary material). In Table 3 the $n_\alpha + n_\beta$ contributions for the various complexes are collected. It is interesting to notice that the n_α and n_β contributions for a given native complex are strongly dependent on the magnetic field setting of the ESEEM spectrum. At first sight this property seems to contradict the proposed two-state model. This behavior is however well understood if one recalls that the ESEEM experiments are subject to effective orientation selection, and the spectra obtained at different fields represent only a limited part of paramagnetic molecules. The excitation bandwidth (Ω_{MW}) of the microwave pulses in orientation-selective ESEEM experiments is comparable to the intrinsic line width of the EPR spectra. Therefore, the number of paramagnetic species n_B monitored at any magnetic field position will be proportional to the EPR intensity at that particular field, $n_B \propto nI_B\Omega_{MW}$ (illustrated with the shaded area under the absorption spectrum of αNO subunits in Figure 1A). Here, *n* is the total number of paramagnetic species, and I_B is the absorption EPR intensity normalized for unit area (i.e., for unit number of paramagnetic species). When two paramagnetic species (i.e., state I and state II) are present in the same sample, and these species have different EPR line shapes $I_{I(II)B}$, then one would expect that their contributions to the ESEEM will vary as $n_{I(II)B} \propto n_{I(II)B}I_{I(II)B}\Omega_{MW}$ at different field positions. Hence, the field-dependent contribution ratio of the two species in orientation-selective experiment can be expressed as

$$(n_{II}/n_I)_B = (n_{II}/n_I)(I_{II}/I_I)_B \qquad (5)$$

where (n_{II}/n_I) represents the real weight ratio of the two species in the sample and the parameter $(I_{II}/I_I)_B$ determines the relative (field-dependent) contribution of the two species. Since the relative intensities of the individual EPR line shapes (I_I and I_{II}) strongly vary at different field positions (illustrated with I_α and I_β in Figure 1A), the parameter $(I_{II}/I_I)_B$ and the relative contribution of the two species $(n_{II}/n_I)_B$ will also vary significantly. It also becomes clear from eq 5 that the relative ratios $(n_{II}/n_I)_{i,B}$ of two different samples *i* and *j* will show a linear relationship since the field-dependent parameter $(I_{II}/I_I)_B$ is divided out. This is demonstrated in Figure 6A where the ratios found for three samples: HbNO(T), (αCO,*β*NO)Hb hybrid, and MbNO, are plotted vs the corresponding ratios of HbNO(R). In other words, each point in this plot relates the (n_β/n_α) ratio of one of the three compounds at a certain magnetic field to the corresponding ratio determined for the HbNO(R) sample. The different slopes in Figure 6A indicate the different relative weights of state II and state I in the samples.

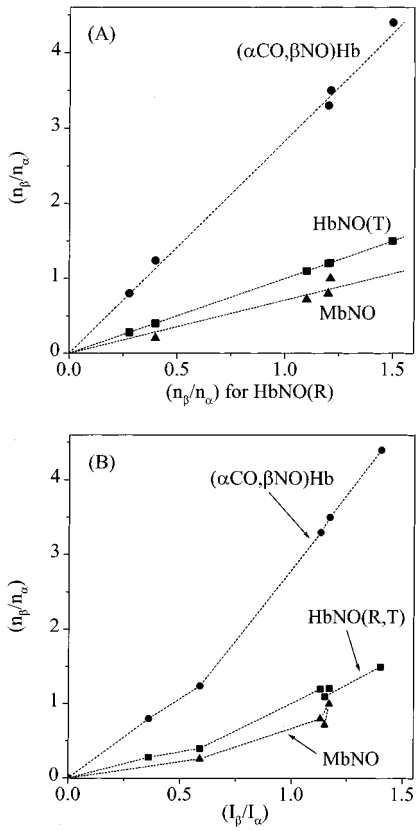

Figure 6. Plots of the $(n_\beta/n_\alpha)_B$ ratios determined for the different samples from the analysis of the ESEEM spectra (A) vs the $(n_\beta/n_\alpha)_B$ ratio for the HbNO(R) sample obtained at the same magnetic field B_0 and (B) vs the $(I_\beta/I_\alpha)_B$ ratio of the normalized intensities of the αNO and *β*NO EPR spectra. The same symbols show the data obtained for the same sample at different applied magnetic fields. The dotted lines in (A) represent for every sample the least-squares linear fit of the experimental points. In (B), the dotted lines simply connect the experimental points of the same sample.

This model is analogous to the two-state model derived from previous EPR and ENDOR results.[12,13] The isolated αNO- and *β*NO chains at low temperatures were shown to be dominated by the rhombic and axial EPR species, respectively, the other samples being represented as a weighted superposition of these two basic forms of spectra. (Note, however, that the EPR signatures of the axial and rhombic spectra were slightly different for α- and *β*-subunits.[13]) In agreement, our present ESEEM observations indicate the two states I and II to be most abundant in the isolated αNO- and *β*NO-chains, respectively. Thus, a qualitative comparison suggests that the "ESEEM-identified" species (states I and II) should be most probably associated with the rhombic and axial EPR states of NO−heme complexes. If so, a correlation between the $(n_\beta/n_\alpha)_B$ ratios derived from ESEEM simulation and the $(I_{II}/I_I)_B$ ratios of the individual EPR intensities should exist (eq 5). Two basic (rhombic and axial) EPR spectra have been derived using factor analysis,[12] and basically the same patterns were recently obtained from a temperature-dependent EPR studies.[13] The derived (rhombic and axial) basic spectra are found to resemble closely the EPR spectra of isolated α(*β*)NO chains. Therefore, as a first approximation, we present in Figure 6B the correlation of the ESEEM ratios (n_β/n_α) vs the (normalized) EPR ratios (I_β/I_α) of isolated *β*(α)NO chains. The data points show a monotonically increasing trend which roughly supports the assignment of ESEEM-identified states I and II to the rhombic and axial EPR components. However, some deviation from the expected linear relationship of eq 5 is definitely observed. This could be ascribed to the effect of using (I_β/I_α) instead of the actual (I_{II}/I_I) ratios. On the other hand, the relation (5) is obviously valid only in the case of two species contributing to EPR and ESEEM spectra. Although both EPR[12,13] and our ESEEM study reveal the evidence of only two major paramagnetic complexes (states I and II), one cannot exclude a minor contribution of some additional species.

The least-squares linear approximates of the experimental points in Figure 6B allow estimations of the equilibrium ratios (n_β/n_α) for the samples investigated (Table 1). The table also lists the corrected n_I/n_{II} contributions based on the estimated compositions of αNO (0.8/0.2) and *β*NO (0.1/0.9) subunits, respectively.

Discussion

Geometry of Two States. The two-state model was first proposed by Morse and Chan, to explain the temperature variation of EPR spectra of NO−myoglobin and nitrosylated model complexes.[12] It assumes an occurrence of two nonequivalent isomers of NO−heme ligation. The isomers were characterized by distinct EPR spectra with axial and rhombic line shapes. Their linear combinations with varied ratios allowed description of the observed temperature dependence of EPR spectra.[12] It was, however, found that the principal postulate of the Morse and Chan analysis is not strictly fulfilled and that the basic axial and, specifically, the rhombic spectra were temperature dependent themselves.[24] A recent X- and Q-band EPR study provided evidence of the two (axial and rhombic) states to occur in both isolated αNO and *β*NO chains of hemoglobin.[13] It appeared practically impossible to describe temperature variation of EPR spectra of both αNO and *β*NO chains simultaneously using the same set of axial and rhombic isomers. The *g*-tensor values of the axial and rhombic species were found closely identical in the two chains at low temperatures and resemble those derived for NO−myoglobin and model NO complexes. This suggests high conservation of the rhombic and axial structures over different NO−heme compounds on one hand combined with spectral diversity within the two states on the other. Moreover, temperature variation was found to induce the axial and rhombic components to change differently in α- and *β*-chains. This was discussed to be due to a different heme compartment at the distal and proximal sides in α- and *β*-chains, resulting in different mobility of the axial heme ligands and/or heme itself when temperature increases. Since the basic axial and rhombic components change with temperature, this explains why the two-state model in its original variant formulated by Morse and Chan, with two temperature-independent axial and rhombic components, fail to reproduce the EPR spectra over the entire temperature interval.

The present ESEEM study provides further evidence of the basic two-state model. The influence of temperature variation of the changes of structural states was experimentally overcome by performing ESEEM measurements at fixed temperature (4.2 K). Under these conditions, orientation-selective three-pulse ESEEM spectra measured over entire EPR line shapes for different NO−heme proteins were successfully synthesized as a linear combination of the spectra from two structural NO−heme states. One of the ESEEM-identified states is found dominating in αNO chains and another in *β*NO chains. On the other hand, EPR study identifies that the rhombic and axial EPR species should dominate in the isolated αNO and *β*NO chains, respectively, at 4.2 K. Therefore, we correlated two ESEEM-identified states with the rhombic and axial NO−heme states derived from EPR experiments. Under this assumption, we were able to quantitatively estimate for the first time the contents of the rhombic and axial states in different NO−heme compounds at this temperature.

Morse and Chan discussed the difference of states I and II in terms of the position of the iron with respect to the heme plane. However, single-crystal EPR work[23−25] suggests that the actual distinctive features are in different Fe−NO bond angles and tilts with respect to the heme normal. Recent single-crystal ENDOR results included the position of the coordinated His F8 nitrogen into the tilted geometry.[26] The single-crystal results correlate well with the state I species in frozen solution. A striking similarity was demonstrated in the *g*-factor values of the rhombic species (2.07, 2.004, 1.97) with those of the "single-crystal" species at low temperature (2.076, 2.002, 1.979), suggesting a close correspondence in their geometries. As was proposed recently for several other NO-ligated hemoglobins and derivatives on the basis of the proton ENDOR data in frozen solutions,[13] we assume for state I a tilted configuration of the axis connecting the His F8 nitrogen, the metal ion, and the nitrosyl nitrogen with respect to the heme plane.[24,26]

The situation for the state II species is more uncertain. In the low-temperature single-crystal EPR studies of MbNO,[50] a minority species was also observed whose *g*-anisotropy was not well characterized. One could tentatively assign this minority single-crystal species to state II. The lack of single-crystal information makes it impossible to draw reliable conclusions about the NO bond configuration in state II only on the basis of EPR measurements since no more information can be obtained from the rather poorly resolved powder EPR spectra (Figure 1). In this respect, the application of the advanced electron paramagnetic resonance techniques (ENDOR, ESEEM) seems to provide the best means of deriving a more detailed picture of the frozen solution NO−heme species.[27,30] State II, which was identified by axial *g*-symmetry ($g_{||} = 1.99$, $g_\perp =$

(50) Nitschke, W. Diploma Thesis, Department of Physics, University of Regensburg, Regensburg, Germany, 1982.

2.03−2.04) in the original frozen solution EPR studies,[12,28] resembles, spectroscopically, the species used in addition to the rhombic state I in the recent delineation of proton ENDOR spectra in the NO−heme compounds.[13] In these studies, state II was identified as a species with a nontilted Fe−NO bond angle. Thus, the rhombic (tilted), and axial (high-symmetry) conformations seem to be an adequate starting point for the analysis of the two Fe(NO)−heme states occurring in native and model systems.

Assignment of ^{14}N ESEEM Signals N1−N3. The ESEEM spectra in our current study show that both state I and II species display features with a number of lines due to coupling with several ^{14}N nuclei. Three groups of nitrogens (N1−N3) were identified from combined ESEEM and HYSCORE analysis (Table 2). The nitrogens N1 of state I with the smallest HFI coupling ($a = 1.75-2.92$ MHz) were preliminarily assigned to pyrrole nitrogens of the porphyrin ring. The assignment was mainly based on the correlation with model complexes with the ^{14}N/^{15}N-labeled imidazole ligands.[30] The two stronger coupled nitrogens N2−N3 of state II ($a = 3.06$ and 5.13 MHz) are still unassigned. They could be due either to a stronger coupled pyrrole nitrogen or to imidazole nitrogens since two histidine residues are found in close vicinity of the heme iron. The proximal (His F8) histidine directly coordinates to iron at the fifth axial position and the distal (His E7) histidine is supposed to form a hydrogen bond with the oxygen of the heme NO−ligand.[27]

The fact that the ESEEM spectra of the NO−Fe(TPP)−imidazole model complexes lack the 5.5-MHz line seems to point to the involvement of a protein-based nitrogen. However, the abundance of state II in the model systems at the low temperatures of the ESEEM experiments (5−10 K) is still uncertain and could perhaps be too low for a noticeable intensity of the 5.5-MHz line; the EPR spectra of the model complex at these temperatures are not very conclusive on this point.[12,13] We will therefore consider all possible candidates for the $|a| = 3.06$ and 5.13 MHz interactions.

First of all, the proximal His F8 histidine must be ruled out. It coordinates to the heme iron by the N_ϵ nitrogen for which the hyperfine constant was determined to be $\cong$17 MHz,[26] which is a magnitude of order out of range for modulation effects.[37] Since usually a ratio of ∼20 applies between the isotropic couplings of coordinated and remote nitrogens,[51] the remote N_δ nitrogen of His F8 is estimated to have $|a| \cong 0.8$ MHz and should also not be considered. The next protein-based candidate is the distal His E7 histidine. The ^{1}H(^{2}D)-ENDOR investigations of NO−heme systems have suggested the presence of a hydrogen bond between the exchangeable N_ϵ proton of His E7 and oxygen of the NO−ligand.[27] Unpaired electron spin density is known to significantly spread over the Fe−NO fragment with nearly 30% residing on the NO ligand.[33] It, therefore, seems reasonable to expect a delocalization of noticeable unpaired electron spin density to the N_ϵ nitrogen of His E7 ($\rho(2s) = 0.20-0.35\%$ corresponds to $a_{iso} = 3-5$ MHz). The pyrrole nitrogens are other likely candidates, being in a different geometry. One could expect that the π-overlap between the d_z^2 orbital of the unpaired electron with the pyrrole system is more favorable in the high-symmetry configuration of state II than in the "tilted" state I leading to a slight increase from 2 to 3−5 MHz of the HFI coupling for pyrrole nitrogens. Therefore, this qualitative consideration of the HFI couplings restricts plausible candidates of N2−N3 nitrogens to amine N_ϵ nitrogen of His E7 and to pyrrole nitrogens.

The next instructive step is to correlate the quadrupole parameter $K^2(3 + \eta^2)$ estimated for the N1−N3 nitrogens (Table 2) with those expected for pyrrole nitrogens 0.63−0.71 MHz^2, and for imine and amine imidazole nitrogens 1.98 and 0.49 MHz^2, respectively.[52,53] Comparison clearly indicates that $K^2(3 + \eta^2)$ of N1 and N2 is close to the value of pyrrole nitrogens while the value for N3 corresponds to the amine nitrogen of the imidazole ring. Therefore, the quadrupole parameters permit a more decisive assignment of both N2 and N3 nitrogens. Couplings N2 are assigned to the pyrrole nitrogens which show a higher HFI coupling ($a = 3.06$ MHz) at the high-symmetry state II conformation as compared to tilted state I. ESEEM signal N3 is most probably associated with the amine N_ϵ of distal His E7, which can form a hydrogen bond with the oxygen of the NO-ligand.

From ENDOR data[13] it was concluded that in both rhombic and axial states a hydrogen bond to the distal histidine is present. The proton hyperfine interaction in the two states differs considerably. It is therefore expected that the nitrogen hyperfine interaction in the rhombic state, like corresponding proton interaction, will be substantially stronger and more anisotropic than that in the axial state, a situation unfavorable for ESEEM detection. This could account for the absence of the N3 signals in the ESEEM of the αNO-chain.

Nitrosyl Hemoglobin Derivatives. For HbNO (R-state), the ESEEM analysis (Table 1) gave the ratio $n_{II}/n_I \cong 1$. This finding is in nice agreement with the EPR results that show the EPR spectra of HbNO(R) at ambient temperature[17] and at 77 K[3] to be the same as would result from a simple sum of the spectra of the isolated αNO and βNO chains. The ratio (∼1:1) corresponds well to the relation of two α-chains and two β-chains per hemoglobin unit, and it seems to suggest an absence of mutual influence of the chains in tetrameric hemoglobin. Although it is conceivable that a cooperative influence of the α(β)-chains in the tetrameric hemoglobin occurs changing the ratios n_{II}/n_I from those in the isolated αNO and βNO-chains but still giving the overall ratio (1:1), the present results from (αNO,βCO)Hb and (αCO,βNO)Hb hybrids as well the previous EPR/ENDOR findings[13] rule out such a possibility. Both hybrids show ratios nearly identical to those of the corresponding separate chains, suggesting thereby virtually no mutual cooperative influence in HbNO tetramer. The small deviation observed for the (αCO,βNO)Hb hybrid could be ascribed to a redistribution of a small amount of NO ligand from β- to α-chains during the preparation and(or) the sample storage.

It is clear from the spectra shown in Figures 2, 3, and 5 that our experiments were performed at high echo intensity and there are no spectral features masked by noise. Therefore, considering now the HbNO(T) sample, we note that the same ESEEM spectra as those of HbNO(R) are obtained, indicating the same balance (1:1) of states I and II. This result does not reflect the changes occurring in hemoglobin upon the quaternary R−T transition which are clearly observed by other, seemingly more "crude" techniques such as CW-EPR[3,18] and optical[2,4] measurements. It is the 5-coordinated NO−heme species that is responsible for the spectral evidence of the R−T transition presented by the two mentioned techniques. On the other hand, it was shown that the 5-coordinated complex remains silent in ESEEM measurements and gives rise only to an unmodulated contribution to the ESE signal.[30]

Nevertheless, the finding that the orientation-selective ESEEM

(51) Dikanov, S. A.; Burgard, C.; Hüttermann, J. *Chem. Phys. Lett.* **1993**, *212*, 493.

(52) Ashby, C. I. H.; Cheng, C. P.; Brown, T. L. *J. Am. Chem. Soc.* **1978**, *100*, 6057.

(53) McCracken, J.; Pember, S.; Benkovic, S. J.; Villafranca, J. J.; Miller, R. J.; Peisach, J. *J. Am. Chem. Soc.* **1988**, *110*, 1069.

spectra of HbNO(R) and HbNO(T) are virtually identical at all magnetic field positions is quite informative. It allows us to conclude, in contrast to previously formulated models,[2,3,28] that only a small part estimated as ~20% of the total amount of NO−heme complexes in HbNO(T) is actually present in the 5-coordinate state. This finding is in accordance with the recent ^{1}H-ENDOR results on αNO(t) chains in their tertiary t-state.[13] Since, in addition, the β-chains are known not to be involved in the formation of the 5-coordinate species, it is obvious that the majority of protein conformations in the T-state of the HbNO molecule represent the same heme−NO group as in the R-state.

Conclusion

The ^{14}N ESEEM experiments presented in this study have provided further insight into the bimodal nature of nitric oxide binding to hemoproteins. The orientation-selected ESEEM spectra of all hemoproteins studied in this research were represented as the contribution of two basic states mainly associated with αNO and βNO chains. These ESEEM results correlate well with the two-conformational model of 6-coordinated nitrosyl−heme complexes proposed earlier from the evaluation of temperature-dependent EPR/ENDOR spectra. Application of 2D HYSCORE spectroscopy to the isolated αNO and βNO chains has allowed us for the first time to characterize the hyperfine couplings with pyrrole nitrogens in the two conformational states. In addition, the interaction with the protein nitrogen assigned to His E7 was detected only for state II. This finding supports the suggestion that the variations of binding geometry in two states of NO−heme is controlled by the heme's protein surrounding.

Although the determined ^{14}N hyperfine couplings are consistent with the earlier proposed conformational models, they cannot serve as a basis for a further refinement of the suggested binding geometries. The complete analysis of ^{14}N ESEEM spectra is complicated because the nitrogen quadrupole interaction produces dominant spectral features and information about the hyperfine couplings with all four pyrrole nitrogens is limited. More detailed studies using ^{15}N-substituted pyrrole nitrogens are necessary to resolve the signals of the individual heme nitrogens which in fact should be nonequivalent. Similar experiments with ion−radicals of chlorophylls[54] and pheophytin[55] have proven to be successful in this respect.

Acknowledgment. S.A.D. acknowledges the receipt of an A. von Humboldt Foundation Research Fellow Award and the hospitality of the Biophysics Department of Saarland University. A.M.T. thanks The Netherlands Organization for Scientific Research (NWO) for supporting his sojourn (1993−1994) at the University of Nijmegen, and the department of Molecular Spectroscopy for its hospitality. This work is part of a program funded by the Deutsche Forschungsgemeinschaft. A.M.T. thanks the Deutsche Forschungsgemeinschaft for the support of his sojourn at Saarland University (March-June 1996).

JA982085Y

(54) Käss, H.; Rauter, J.; Bönigk, B.; Höfer, P.; Lubitz, W. *J. Phys. Chem.* **1995**, *99*, 436.

(55) Deligiannakis, Y.; Rutherford, A. W. *J. Am. Chem. Soc.* **1997**, *119*, 4471.